

The Effect of Jointing in Massive Highly Interlocked Rockmasses Under High Stresses by Using a FDEM Approach

Ioannis Vazaios¹, Nicholas Vlachopoulos², and Mark S. Diederichs

Abstract

In deep underground mines and deep infrastructure tunnels, spalling and strain bursting are among the most common failure mechanisms observed and reported in massive rockmasses under high stresses. Therefore, the need to be able to estimate such conditions and counter them with an economic and effective design is rising. Part of the common practice is the use of computer packages involving numerical methods based on continuum approaches. However, the failure mechanisms involved and the rockmass response observed are often difficult to capture by employing such methods and usually discontinuum approaches are better suited for this task. Additionally, discrete structures observed within the rockmass in situ, such as joints and other discontinuities, can be explicitly incorporated into the numerical model in order to investigate their effect on the overall rockmass response during an underground excavation and adjust the design if necessary. In this study, the presence of joints and their effect on the response of a hard rockmass under a high stress regime during an excavation is examined by employing a FDEM (Finite-Discrete Element Method) approach. The setup of the numerical model is based on the URL (Underground Research Laboratory) Test Tunnel located in Pinawa, Manitoba, Canada and a Discrete Fracture Network (DFN) model is

implemented in order to simulate the impact of joints on brittle failure. Numerical results show that the presence of joints increases the intensity and evolution of the damage during the excavation.

Keywords

Finite-Discrete element method (FDEM) • Brittle failure • Tunnelling

1 Introduction

Within hard, massive rockmasses, brittle behaviour can cause significant problems in deep tunnelling (Kaiser and McCreath 1994; Lee et al. 2004; Diederichs et al. 2004), similarly to deep mining excavations (Hoek 1968; Hoek and Brown 1980). Spalling and strain bursting are the most common failure mechanisms observed in hard rock excavations under high stress regimes, and they are associated with complex failure mechanisms which are usually quite difficult to simulate numerically by employing continuum mechanics approaches. Additionally, challenges arise when pre-existing joints are present and they need to be incorporated into the numerical model. In such cases, discontinuum modelling techniques are usually more suitable for simulating the associated fracture phenomena that occur as a result of the joints and the brittle rock response.

For the purposes of this study, the short term mechanical response of hard rock excavations is investigated by applying a finite-discrete element method (FDEM) technique implemented into the Irazu software (Geomechanica 2017). The setup of the numerical model is based on the URL (Underground Research Laboratory) Test Tunnel located in Pinawa, Manitoba, Canada and a Discrete Fracture Network (DFN) model is implemented in order to simulate the impact of joints on brittle failure.

I. Vazaios (✉) · N. Vlachopoulos · M. S. Diederichs
Department of Geological Sciences and Geological Engineering,
Queen's University, Kingston, Canada
e-mail: ioannis.vazaios87@gmail.com

N. Vlachopoulos
e-mail: vlachopoulos-n@rmc.ca

M. S. Diederichs
e-mail: diederim@queensu.ca

N. Vlachopoulos
Department of Civil Engineering, Royal Military College of
Canada, Kingston, Canada

2 The Geological Setting

2.1 Intact Material Properties

For the development of the numerical model, the mechanical properties of the intact material were required to be representative of this of a hard rock which could demonstrate brittle behaviour. In order to achieve this, the well documented case of the Lac du Bonnet (LdB) granite, located in Manitoba, Canada, was selected (Martin 1994; Martin et al. 1997; Hajiabdolmajid et al. 2002, 2003). The LdB granite is a relatively undifferentiated, massive rock of Precambrian age with a relatively uniform texture and composition (Chandler 2003). The mechanical properties of the LdB granite are listed in Table 1.

2.2 Discontinuity Geometrical Properties

The LdB granite has been characterized as a relatively undisturbed rockmass (Hajiabdolmajid 2001), and for the purposes of this study it is considered as a fractured free medium, an assumption supported by field observations as well (Martin 1994). In order to investigate the effect of pre-existing joints within a brittle, hard rockmass, structural data obtained from an unsupported tunnel is used to generate a stochastic network of joints.

The discontinuity data required were acquired by utilizing point-clouds obtained from LiDAR (Light Detection and Ranging) scanning of an unlined 10 m section of a railway tunnel located in Brockville, Ontario, Canada (Fig. 1a). The point cloud was meshed to create a 3D surface model and discontinuity mapping was conducted (Fig. 1b–d) using Polyworks, which is a multipurpose range imaging processing package (Innovometrics 2016), in order to determine the orientation of the identified sets and their fracture intensity (Vazaios et al. 2017). The discontinuity geometrical properties are listed in Table 2.

Table 1 Experimental values (average value and range) of the mechanical properties of the intact Lac du Bonnet granite (Martin 1994)

Mechanical property	Value
Young's modulus E (GPa)	69.0 ± 5.8
Poisson's ratio ν	0.22 ± 0.04
Unconfined compressive strength UCS (MPa)	213 ± 20
Tensile strength σ_t (MPa)	9.3 ± 1.3
Cohesion C (MPa)	30
Friction angle ($^\circ$)	59

3 DFN Generation

The collection of discontinuity data described in Sect. 2.2 served as input for the generation of a stochastic discontinuity network which was used to create the joint features which were incorporated into the numerical model. In order to create the utilized DFN, the DFN generator MoFrac (Mirarco 2015) was used. Initially, a master volume is determined in order to generate the DFN. Random seeds within this volume are created and the employed propagation algorithm creates discontinuity surfaces (consisting of a triangular mesh) using the measured orientation and fracture intensity. Additionally, the mapped traces are used to create deterministic discontinuities at the specific locations that they were mapped. For more information the reader is referred to Vazaios et al. (2017).

The generated DFN model used in this study consists of a volume of $60 \times 60 \times 60$ m (Fig. 2a), in order to minimize the effect of possible boundary effects, and in order to be validated 10 random mapping windows with an equivalent area of 56 m^2 were created. Within these mapping windows, the traces were mapped and their lengths were measured for every one of the three sets in order to ensure that they follow the obtained distributions from the traces mapped within the LiDAR data (Fig. 2b). Once the DFN model was validated, a cross-section of it was extracted in order to be imported into the numerical model.

4 Development of the FDEM Numerical Model

4.1 Model Geometry, Boundary Conditions, Stress State and Excavation Sequence

The main geometrical features of the model are illustrated in Fig. 3. The model, which was built in Irazu, is made of 3-node triangular elements. It consists of a 3.50 m diameter

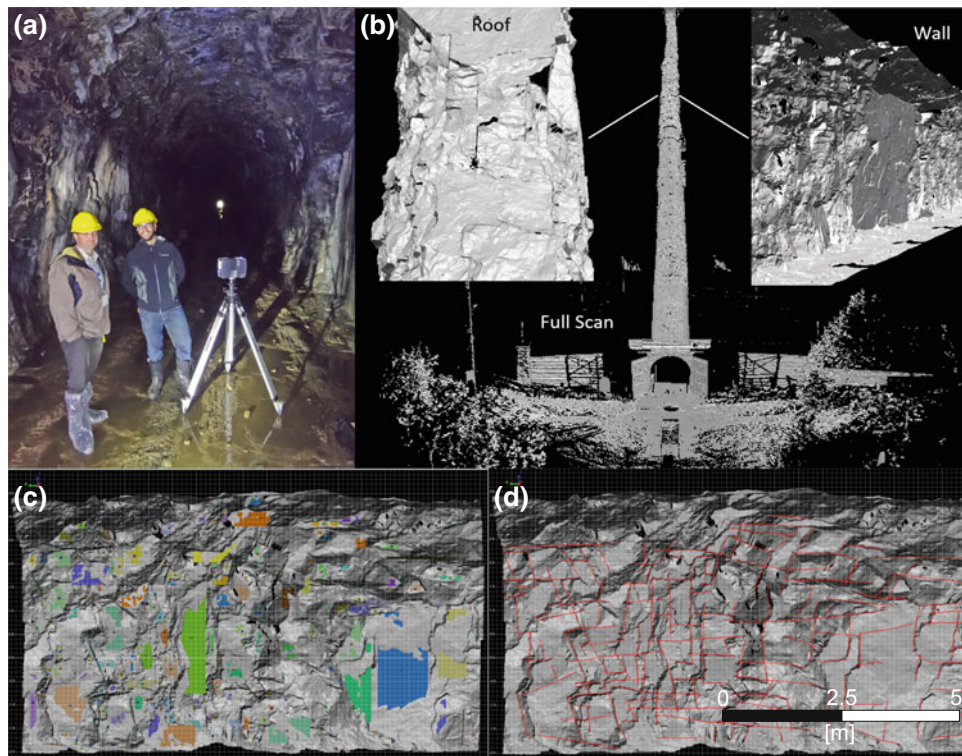


Fig. 1 a Terrestrial laser scanning conducted in an unlined section of the Brockville Railway Tunnel, Ontario, Canada. b 3D surface model of the tunnel created from the acquired LiDAR data. Discontinuity surface (c) and discontinuity trace (d) “virtual” mapping performed at a 10 m section of the tunnel

Table 2 Discontinuity geometrical data of an unlined 10 m section of the Brockville railway tunnel (Vazaios et al. 2017)

Set	Dip (°)	Dip direction (°)	Mapping area (m ²)	Trace length (m)	Areal fracture intensity (m/m ²)
1	88	285	60	71.03	1.18
2	12	077	54	91.61	1.70
3	77	207	54	62.93	1.17

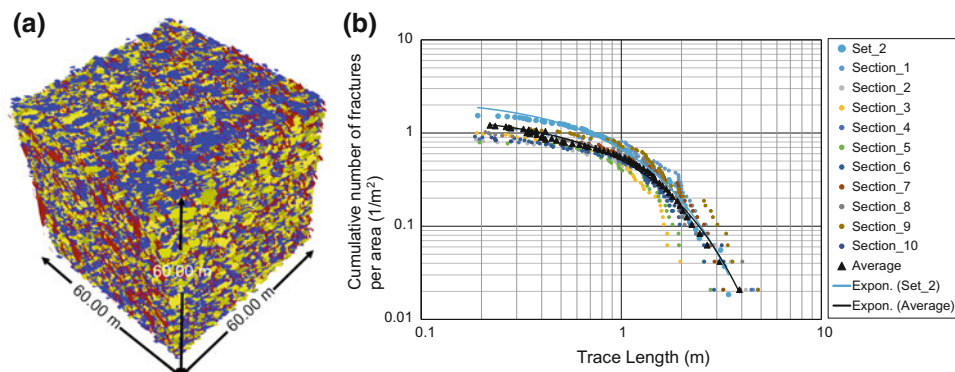


Fig. 2 a DFN model generated by using LiDAR data collected from a 10 m unlined section of the Brockville Railway tunnel. b Cumulative discontinuity trace length distributions created after field data (blue curve) and data obtained from the generated DFN model (black curve)

Fig. 3 Tunnel model configuration (geometry and stress state) created in Irazu. The different mesh domains within the model are highlighted with yellow dashed squares, showing the element size variation and transition between the excavation area (area of interest) and the model boundaries. The pre-existing discontinuities originating from the implemented DFN model are coloured red

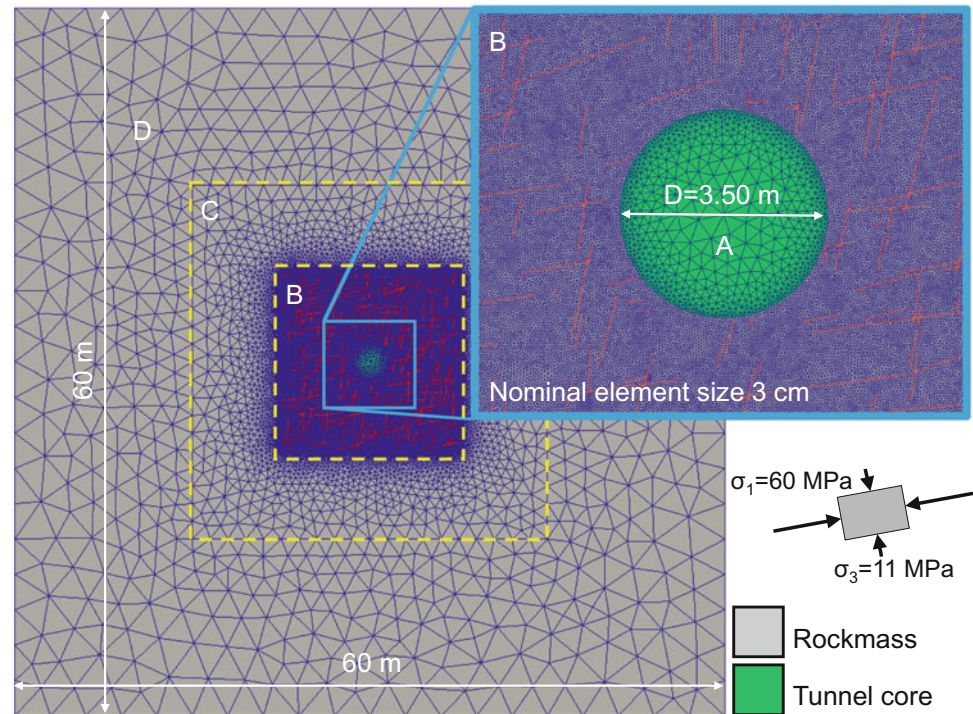


Table 3 The URL Test Tunnel stress tensor (Martin et al. 1997) and the assigned stress field to the FDEM model. All listed stresses are compressive

	Stress component	Magnitude (MPa)
URL test tunnel	σ_1	60 ± 3
	σ_2	45 ± 4
	σ_3	11 ± 4
FDEM model	σ_{xx}	58.0
	σ_{yy}	13.0
	τ_{xy}	9.2

tunnel, which corresponds to the diameter of the URL Test Tunnel and a 60×60 m square domain which is divided into four different sub-domains A, B, C and D with nominal element sizes 0.50, 0.03, 1.50 and 4.00 m respectively. Within Domain B, the mesh was refined in order to be able to capture the brittle fracturing response that the rockmass was expected to demonstrate as a result of the excavation. The model was meshed by using Gmsh (Geuzaine and Remacle 2009) and an unstructured Delaunay triangulation scheme was applied in order to minimize the effect of the mesh topology on the fracturing processes, as suggested by Mahabadi et al. (2012) and Lisjak et al. (2014). The model containing the incorporated DFN model consists of approximately 615,000 elements and the DFN-free model consists of 600,000 elements respectively.

The greater dimension of the model was selected to be 60 m (30 m from the centre of the excavation at each

direction) in order to minimize possible boundary effects. Additionally, the displacements were fixed in the X and Y direction and an absorbing boundary condition was employed. Finally, a constant stress field condition was applied to the FDEM model. The stress components used are listed in Table 3 and they correspond to the stresses measured at the URL Test Tunnel.

Following the establishment of the model geometry, a geostatic stress field was applied and the excavation of the tunnel was performed sequentially by decreasing the deformation modulus of the excavated material (softening of the core) from its initial value to zero (Vlachopoulos and Diederichs 2014). The geostatic stage of the model was established within 500,000 steps, followed by 4,000,000 excavation steps during which the softening of the core took place. Finally, 3,000,000 time steps were performed in order to establish static equilibrium conditions after the completion of the excavation.

4.2 Model Deformability and Strength Parameters

The primary form of damage within hard rockmasses is that of extensile failure, with the internal tensile strength of the geomaterial controlling the fracturing processes, especially under low confinement conditions around underground excavations in high stress environments (Diederichs 2007).

Such fracturing processes at low confinement stresses can be modelled by applying a FDEM approach in which crack initiation and propagation are explicitly simulated by adopting a cohesive-zone approach. This technique allows for the progressive failure of rock materials through the strength degradation of 4-node interface elements that are installed between the 3-node triangular elements (Lisjak et al. 2015), and therefore the use of a macroscopic failure criterion (Mohr-Coulomb, Hoek-Brown etc.) is not required. An explicit time integration scheme is employed in order to solve the motion equations of the discretized system and it updates the nodal coordinates at each simulation step (Lisjak et al. 2015).

The deformability of the system prior to any fracturing depends on the elastic properties of the triangular elements which are assigned a Young's modulus E and a Poisson's ratio ν . While the interface elements are not supposed to deform before their strength is exceeded, the time-explicit formulation of the FDEM requires a finite cohesive stiffness. This artificial stiffness is introduced in the system by defining normal, tangential and fracture penalty values p_n , p_t , and p_f respectively (Munjiza 2004; Mahabadi 2012).

The strength of the interface elements is determined based on their tensile strength and their shear strength. The response in tension of the interface elements is governed by their assigned tensile strength f_t and the fracture energy in

tension G_I . Similarly, their response in shearing is governed by the assigned cohesion c , the internal friction angle φ expressed as a frictional coefficient μ , and the fracture energy in shear G_{II} (Lisjak 2013).

The deformability and strength parameters adopted in this study were based on a calibrated model procedure of the URL Test Tunnel. The calibrated model replicates the brittle behaviour of the LdB granite observed during the excavation of the tunnel and the extent of the damaged material, as a result of the spalling processes taking place in a fracture free environment. For the FDEM model containing the DFN model, the discontinuities were assumed to be purely frictional for simplicity. The deformability and strength parameters used in this study are listed in Table 4.

5 Results and Discussion

In order to investigate the effect of pre-existing discontinuities on the failure mechanisms of hard, brittle rockmasses and the extent of the damaged zone around an excavation at great depths, the two numerical models were compared for various stages of the excavation process.

In Fig. 4a–d the magnitude of the deviatoric stresses is illustrated along with the fractures that have been formed as a result of the yielding of the interface elements due to the changes of the stress regime because of the excavation. In Fig. 4a, b, both models are captured before the initiation of any fracturing as a result of the excavation. Stress concentrations occur at the crown and the floor of the excavation at approximately the same locations for both models, as a result of the advancing face. However, it can be observed that the formation and the magnitude of the stress contours are not exactly the same due to the presence of the pre-existing

Table 4 Input parameters for the FDEM simulation using Irazu

Parameter	Value
Young's Modulus E (GPa)	65
Poisson's ratio ν	0.18
Viscous damping factor	1.0
Normal contact penalty p_n (GPa m)	650
Tangential contact penalty p_t (GPa/m)	650
Fracture penalty p_f (GPa)	650
Friction coefficient μ	1.7
Cohesion c (MPa)	50
Tensile strength f_t (MPa)	10
Mode I fracture energy G_I (N/m)	300
Mode II fracture energy G_{II} (N/m)	1900
Discontinuity friction coefficient μ_f	0.7

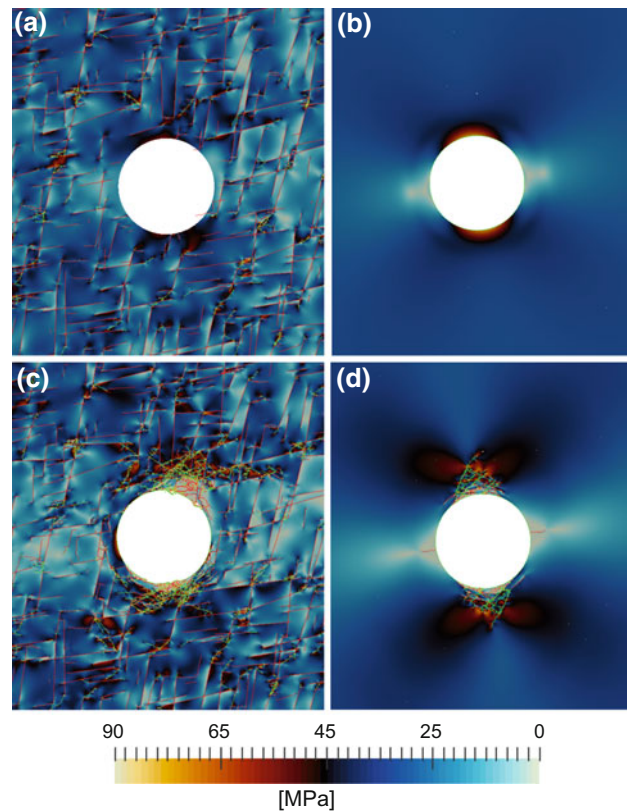
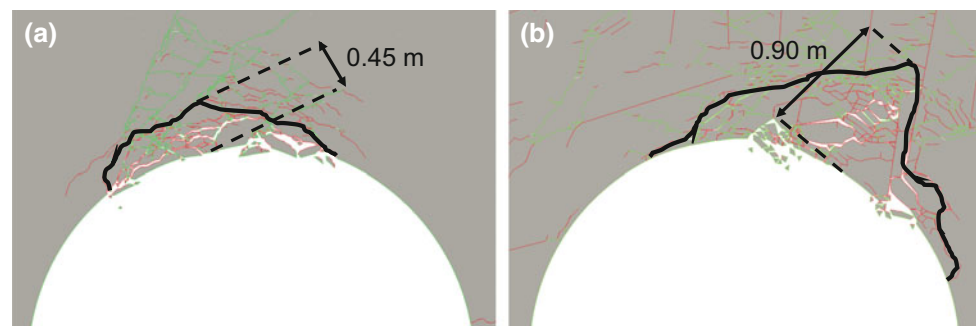


Fig. 4 Deviatoric stress contour plots for the **a** “fractured” model and **b** “intact” model prior to fracture initiation, and **c** the “fractured” and **d** “intact” model when fractures have propagated. Shear fractures are coloured green and tensile fractures are coloured red

Fig. 5 Extent of collapsed material (black curve) in **a** the FDEM and **b** the FDEM-DFN models. Tensile fractures are highlighted red and shear fractures are highlighted green



planes of weakness in the FDEM-DFN model, herein called “fractured” model. More specifically, in the “fractured” model the resultant stresses appear to have a lower magnitude than in the “intact” model. Furthermore, while stress induced fractures around the excavation are absent, it can be seen that stress concentrations at the tips of the pre-existing joints cause the initiation of fracturing and fracture interaction away from but still within the vicinity of the excavation. In Fig. 4c, further advancement of the face is leading to the interaction between stress induced fractures and pre-existing discontinuities in the “fracture” model. On the contrary, in

Fig. 4d, in the “intact” model fractures are free to propagate and their formation is dictated solely by the stresses present.

By focusing on the crown of the excavation in both models (Fig. 5), it can be observed that in the case of the “intact model” the high compressive stresses concentrating at this specific location result in the extensile failure of the material (Fig. 5a). The extensile stress induced fractures follow approximately the trajectories of the high magnitude compressive tangential stresses around the excavation boundary. That leads to the formation of a “v-shaped” notch type failure, similar to the one observed in the field at the

URL Test Tunnel (Martin et al. 1997; Diederichs 2007), as the tensile strength of the rockmass is exceeded. Additionally, the notch is formed at an angle relative to the vertical axis of the model, which is consistent with the stress tensor described in Table 3, with the extent of the collapsed material being approximately 0.45 m.

This is not the case, however, for the “fractured” model. As illustrated in Fig. 5b, the pre-existing discontinuities present re-direct the excavation induced stresses resulting in a failed area that is rotated relative to the one developing in the “intact” model. More specifically, a sub-horizontal joint located at the crown of the tunnel acts as a stress barrier preventing the formation of the notch, and it forces the stress induced fractures to move to the right. As the stress induced fractures propagate further, the sub-vertical joints “trap” the formed cracks and lead to the containment of the undergoing fracturing processes, with the extent of the collapsed material being approximately 0.90 m. While the manifestation of the failed material and the extent of the damage occurring are different between the “intact” and the “fractured” configurations, it has to be noted that the main failure mechanism in both cases is brittle, extensile failure. As seen in Fig. 5b, tensile fractures are propagating in the intact part of the rockmass encountered between the sub-vertical joints, once the tensile strength of the rockmass has been exceeded, hence leading to the collapse of the material.

6 Conclusions

In this study, the effect of pre-existing discontinuities on the response of brittle, hard rockmasses by employing a hybrid FDEM-DFN approach was investigated. From the obtained numerical results it becomes evident that while the dominant damage mechanism is extensile fracturing in both examined scenarios, the presence of pre-existing joints increases the intensity of the damage sustained to the rockmass. Additionally discontinuities can act as stress barriers and redirect the evolution of the inflicted damage on the rockmass, which is controlled by the joint network geometry.

Acknowledgements The authors would like to thank the Nuclear Waste Management Organization of Canada (NWMO), the Natural Sciences and Engineering Research Council of Canada (NSERC), the Department of National Defense (Canada) and the RMC Green Team for funding this work. Additionally, the authors would like to thank Dr. Omid K. Mahabadi and Dr. Andrea Lisjak (Geomechanica Inc.) for their continuous support.

References

- Chandler, N.A.: Twenty years of underground research at Canada’s URL. In: WM’ 03 conference Tucson AZ (2003)
- Diederichs, M.S., Kaiser, P.K., Eberhardt, E.: Damage initiation and propagation in hard rock during tunnelling and the influence of near-face stress rotation. *Int. J. Rock Mech. Min. Sci.* **41**(5), 785–812 (2004)
- Diederichs, M.S.: The 2003 Canadian geotechnical colloquium: mechanistic interpretation and practical application of damage and spalling prediction criteria for deep tunnelling. *Can. Geotech. J.* **44**(9), 1082–1116 (2007)
- Geomechanica Inc.: Irazu 2D Geomechanical simulation software, version 3.0 (2017)
- Geuzaine, C., Remacle, J.F.: Gmsh: a three-dimensional finite element mesh generator with built-in pre- and post-processing facilities. *Int. J. Numer. Meth. Eng.* **79**(11), 1309–1331 (2009)
- Hajiabdolmajid, V.R.: Mobilization of strength in brittle failure of rock. Ph.D. Thesis, Department of Mining Engineering, Queen’s University, Kingston, Canada (2001)
- Hajiabdolmajid, V.R., Kaiser, P.K., Martin, C.D.: Modelling brittle failure of rock. *Int. J. Rock Mech. Min. Sci.* **39**(6), 731–741 (2002)
- Hajiabdolmajid, V.R., Kaiser, P.K., Martin, C.D.: Mobilized strength components in brittle failure of rock. *Geotechnique* **53**(3), 327–336 (2003)
- Hoek, E.: Brittle failure of rock. In: Stagg, K.G., Zienkiewicz, O.C. (eds.) *Rock mechanics in engineering practice*, pp. 99–124. Wiley, London (1968)
- Hoek, E., Brown, E.T.: *Underground excavations in rock*. Institute of Mining and Metallurgy, London (1980)
- Innovometrics: Polyworks V 11.0.4, Quebec City: Innovometrics (2016)
- Kaiser, P.K., McCreath, D.R.: Rock mechanics considerations for drilled or bored excavations in hard rock. *Tunn. Undergr. Space Technol.* **9**(4), 425–437 (1994)
- Lee, S.M., Park, B.S., Lee, S.W.: Analysis of rockbursts that have occurred in a waterway tunnel in Korea. *Int. J. Rock Mech. Min. Sci.* **41**, 911–916 (2004)
- Lisjak, A.: Investigating the influence of mechanical anisotropy on the fracturing behaviour of brittle clay shales with application to deep geological repositories. Ph.D. thesis, University of Toronto, Toronto, Canada (2013)
- Lisjak, A., Grasselli, G., Vietor, T.: Continuum–discontinuum analysis of failure mechanisms around unsupported circular excavations in anisotropic clay shales. *Int. J. Rock Mech. Min. Sci.* **65**, 96–115 (2014)
- Lisjak, A., Garitte, B., Grasselli, G., Müller, H.R., Vietor, T.: The excavation of a circular tunnel in a bedded argillaceous rock (Opalinus Clay): short-term rock mass response and FDEM numerical analysis. *Tunn. Undergr. Space Technol.* **45**, 227–248 (2015)
- Mahabadi, O.K.: Investigating the influence of micro-scale heterogeneity and microstructure on the failure and mechanical behaviour of geomaterials. Ph.D. thesis, University of Toronto, Toronto, Canada (2012)
- Mahabadi, O.K., Lisjak, A., Grasselli, G., Munjiza, A.: Y-Geo: a new combined finite-discrete element numerical code for geomechanical applications. *Int. J. Geomech.* **12**, 676–688 (2012)

- Martin, C.D.: The strength of massive Lac du Bonnet granite around underground openings. Ph.D. thesis, University of Manitoba, Winnipeg, Manitoba, Canada (1994)
- Martin, C.D., Read, R.S., Martino, J.B.: Observations of brittle failure around a circular test tunnel. *Int. J. Rock Mech. Min. Sci.* **34**(7), 1065–1073 (1997)
- MoFrac software version alpha: MIRARCO Mining Innovation, www.mofrac.com (2015)
- Munjiza, A.: The combined finite-discrete element method. Wiley, Chichester, West Sussex, England (2004)
- Vazaios, I., Vlachopoulos, N., Diederichs, M.S.: Integration of lidar-based structural input and discrete fracture network generation for underground applications. *Geol. Geotech. Eng.* **35**(5), 2227–2251 (2017)
- Vlachopoulos, N., Diederichs, M.S.: Appropriate uses and practical limitations of 2D numerical analysis of tunnels and tunnel support response. *Geotech. Geol. Eng.* **32**(2), 469–488 (2014)